Catalysis Letters, Vol. 116, Nos. 3–4, August 2007 (© 2007)
DOI: 10.1007/s10562-007-9099-4

Preparation and catalytic performance of Co_3O_4 catalysts for low-temperature CO oxidation

Yong-Zhao Wang, Yong-Xiang Zhao,* Chun-Guang Gao, and Dian-Sheng Liu*

School of Chemistry and Chemical Engineering, Institute of Advanced Chemistry, Shanxi University, Taiyuan 030006, China

Received 25 February 2007; accepted 17 March 2007

Without use of any surfactant or oxidant, a series of Co_3O_4 catalysts have been prepared from cobalt nitrate aqueous solution via a very simple liquid-precipitation method with ammonium acid carbonate followed by calcination at various temperatures. The catalytic performance of the Co_3O_4 for CO oxidation has been studied with a continuous flowing laboratory microreactor system. The results show that the CO conversion of all the samples can reach 100% at ambient temperature. The catalyst calcined at 300 °C is able to maintain its activity for CO complete oxidation more than 500 min at 25 °C and about 240 min even at −78 °C. High reaction temperature results in a high catalytic stability, while the catalytic stability decreases with further increasing the reaction temperature. Characterizations with X-ray powder diffraction and transmission electron microscopy suggest that all the samples exist as a pure Co_3O_4 phase with the spinel structure, the samples are apt to aggregate and the specific surface area gradually decreases with increasing the calcination temperature, which directly leads to the decrease of catalytic stability. Furthermore, the amount of active oxygen species measured by CO titration experiments appears to be critical for catalytic performance.

KEY WORDS: Co_3O_4; liquid-precipitation; low-temperature CO oxidation; active oxygen species.

1. Introduction

The low-temperature catalytic oxidation of CO has become an important research topic over the years due to its many potential areas of applications [1–9]. Particularly, these applications include air-purification devices for respiratory protection, pollution control devices for reducing industrial and automotive emissions, closed-cycle carbon dioxide lasers, removing trace quantities of CO from the ambient air in sealed cabins such as submarines and space crafts on long duration missions and carbon monoxide gas sensors. Recently, the selective CO oxidation in the fuel cell at low temperature also becomes important. Precious metal catalysts, such as Pd/CeO_2–TiO_2, Pd/NaZSM-5, Pt/CeO_2 and Sn–Pt/SiO_2 [10–13], especially many gold-base catalysts supported on different materials have been studied for CO oxidation and show high catalytic activities [14–20]. However, the sensitivity of precious metals to sulfur poisoning and their high cost have long motivated the search for substitute catalysts including various transition metal oxides [21–37].

As a promising candidate of precious metal catalysts, cobalt oxide catalysts have attracted considerable attention because of not only its high activity for CO and hydrocarbon oxidation [26, 38], but also its use in the Fischer–Tropsch synthesis [39], NO decomposition [40], and ammonia oxidation [41]. Particularly, the low-temperature CO oxidation over Co_3O_4 has been studied by several groups. Jia *et al.* [27] prepared nanometer Co_3O_4 using dodecylbenzene sulfonic acid sodium salt (DBS) as the surfactant and found it was able to oxide completely CO at low temperature, but without using DBS the catalytic activity became very poor. Lin *et al.* [28–29] and Wang *et al.* [30] reported the synthesis of Co_3O_4 by the precipitation-oxidation method with hydrogen peroxide as the oxidant combined with the temperature program reduction technique. Wang *et al.* found that the Co_3O_4 prepared by precipitation-oxidation method with hydrogen peroxide exhibited higher activity than that prepared by impregnation or hydrothermal due to the use of oxidant. Yu Yao [26] studied kinetic parameters and Jansson [32] studied the deactivation for the reaction over Co_3O_4 obtained from the decomposition of Co_2O_3 or commercial Co_3O_4, but the activity or stability was not good. From the results of the literatures it can be seen that the surfactant or oxidant is necessary to obtain a Co_3O_4 catalyst with high catalytic activity and stability. However, about the above mentioned method there are many disadvantages such as the second pollution due to elimination of surfactant, the complicated process of operation and the cost of surfactant and oxidant.

---

*To whom correspondence should be addressed.
E-mails: dsliu@mail.sxu.edu.cn; yxzhao@sxu.edu.cn

In this paper, without use of any surfactant or oxidant, the Co_3O_4 catalysts with high catalytic activity for low-temperature CO oxidation were obtained via better control of various preparation parameters in liquid-precipitation process. Influences of activity test condition on the catalytic performance were also discussed. The samples were characterized by means of X-ray powder diffraction (XRD), Transmission electron microscopy (TEM), N_2 adsorption-desorption, Infrared spectroscopy (FT-IR) and CO titration. The results of this physicochemical characterization were discussed in relation to the exhibited catalytic performance of the Co_3O_4 catalysts.

2. Experimental

2.1. Preparation of catalysts

A Co_3O_4 sample was prepared via a liquid-precipitation method in an aqueous solution. 30 ml of 4.0 M cobalt nitrate solution was added drop by drop to 30 ml of 2.0 M ammonium acid carbonate solution under constant stirring at 25 °C. The temperature was then raised to 30 °C and maintained for 3 h. The final pH is about 8.0. The resulting suspension was filtered and the obtained precipitate was washed several times with deionized water, and then it was dried in air at 110 °C for 12 h. Finally, the samples were calcined at 250, 300, 400 and 600 °C in flowing air for 3 h, respectively. The obtained samples were coded as LPC-T, where T refers to the calcination temperature.

2.2. Characterization of catalysts

XRD patterns of the samples were recorded on a Rigaku D/MAX-RB X-ray diffractometer with a target of Cu K_α operated at 50 kV and 60 mA with a scanning speed of 0.5 °/min and a scanning angle (2θ) range of 15–75 °. Average particle sizes of the Co_3O_4 samples were measured from X-ray line broadening analysis (XLBA) using the well-known Scherrer equation [42]:

$$d = \frac{0.89\lambda}{B(2\theta)\cos\theta}$$

N_2 adsorption–desorption isotherms at −196 °C were determined using CE SORPTOMATIC 1990 SERIES instrument. Prior to the sorption experiments, the samples were degassed under vacuum at 150 °C for 12 h. The specific surface area was determined from the nitrogen adsorption isotherm.

The infrared spectra (FT-IR) of the samples were obtained on a 1730 Infrared Fourier Transform Spectrometer (Perkin–Elmer) in the range of 450–1500 cm^{-1} with a resolution of 4 cm^{-1}. One milligram of each powder sample was diluted with 200 mg of potassium bromide (KBr) powder.

Transmission electron microscopy (TEM) measurements were carried out by using Hitachi H-800 TEM operated at 80 kv. Samples for TEM were dispersed by ultrasonic in acetone followed by deposition of the suspension onto a standard Cu grid covered with a holey carbon film.

The amount of active oxygen species on the catalysts was measured by CO titration at 25 °C. 100 mg of sample was loaded in a 4 mm i.d. quartz microreactor and heated in flowing air (30 mL min^{-1}) at 200 °C for 30 min, then cooled to 25 °C in flowing N_2 (30 mL min^{-1}). 1 ml of 3% CO/N_2 was injected with a syringe repeatedly until no CO_2 was observed in the effluent gases. The pulses were performed at intervals of 5 min. The amount of active oxygen species was calculated from the amount of CO_2 obtained during the pulse. The analysis of the effluent gases (CO and CO_2) was performed with an on-line gas chromatograph equipped with a 3 m column packed with carbon molecular sieve, a methanator and a Flame Ionization Detector (FID). In order to enhance the sensitivity of the detection, CO and CO_2 were converted to CH_4 by the methanator at 360 °C before entering into the FID. The minimum detection level was ca. 10 ppm.

2.3. Apparatus and method for activity test

The measurements of catalytic activity for low-temperature CO oxidation were carried out in a continuous flow laboratory microreactor under atmospheric pressure. The microreactor was a 8 mm i.d. quartz u-tube, and a thermocouple enveloped in glass was set into the catalyst bed to measure the temperature. The samples were sieved to 40–60 mesh so that pressure drop and concentration and temperature gradients over the catalyst bed were negligible. 300 mg of catalysts was used for each run. The feed gases adjusted by mass flow controllers consisted of 0.5vol% CO, 14.4vol% O_2 and 85.1vol% N_2 passed through the catalyst bed with a total flow rate of 20 mL min^{-1}. Quantitative analysis of CO and CO_2 was the same as the method described in the CO titration experiment.

Prior to all catalytic experiments the catalysts were pretreated in flowing air at 200 °C for 30 min to yield clean surface and then cooled in the absence of flowing air. During the test, pretreatment and reaction gases were dried fully through the molecular sieve and silica gel. Control at low temperature (−78, −20 and 0 °C) was achieved by methanol–dry ice, ice–salt or ice–water mixture, respectively. For higher than room temperature a temperature controller was used.

The CO conversion was calculated based on the CO consumption as follows:

$$\% \text{ of Conversion of CO} = \frac{[\mathrm{CO}]_{\mathrm{in}} - [\mathrm{CO}]_{\mathrm{out}}}{[\mathrm{CO}]_{\mathrm{in}}} \times 100$$

3. Results and discussion

3.1. *Characterization of catalysts*

The XRD patterns of a series of catalysts obtained at different calcination temperatures are presented in figure 1. Powder XRD peaks of the cobalt oxide are well consistent with the data of the JCPDS file of Co_3O_4 with cubic phase. It is clear that Co_3O_4 is the only phase after the decomposition of the precipitate at 250, 300, 400 and 600 °C, and no diffraction peak other than those of Co_3O_4 are present. All the samples are well crystallized and the degree of crystallinity increases gradually with increasing the calcination temperature. The average particle sizes, i.e. XLBA sizes, according to the (311) diffraction pattern of crystalline Co_3O_4, can be calculated using the Scherrer equation, which is in broad agreement with our TEM observation (will be presented shortly), listed in the third column of table 1. From the results it can be seen that the order of particle size is: LPC-600(62 nm) > LPC-400(20 nm) > LPC-300(10 nm) > LPC-250 (8 nm).

Table 1 shows the physicochemical properties of the samples obtained at calcination temperature ranging from 250 to 600 °C. The specific surface area (S_{BET}, m^2g^{-1}) is listed in the second column of table 1. Calcination of the sample at 250 and 300 °C had a small effect on the specific surface area (61–54 m^2g^{-1}). However, it was seen that the specific surface area was reduced dramatically to 30 m^2g^{-1} (LPC-400) and 9 m^2g^{-1} (LPC-600) when the calcination temperature was further increased to 400 and 600 °C, respectively. The decrease of the specific surface area is probably due to the growth and aggregation of the Co_3O_4 nanoparticles with the increasing calcination temperature, which is also agreement with our TEM observation (will be presented shortly).

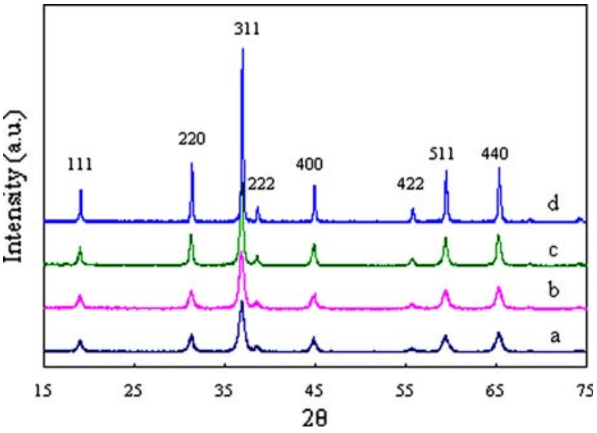

Figure 1. XRD patterns of Co_3O_4 calcined at different temperatures: (a) 250 °C; (b) 300 °C; (c) 400 °C and (d) 600 °C.

Table 1

S_{BET}, XLBA size, TEM size, Amount of active oxygen species and stability on CO oxidation of Co_3O_4 calcined at different temperatures

Sample	S_{BET} (m^2g^{-1})	XLBA (nm)	TEM (nm)	Amount of active oxygen species (μ molg^{-1})	Stability (nm)
LPC-250	61	8	5–10	99	240
LPC-300	54	10	8–13	144	500
LPC-400	30	20	18–22	91	230
LPC-600	9	62	44–80	21	50

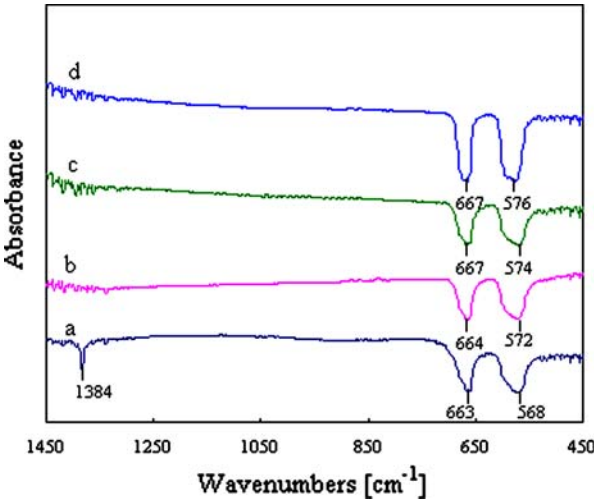

Figure 2. FTIR spectra of Co_3O_4 calcined at different temperatures in KBr: (a) 250 °C; (b) 300 °C; (c) 400 °C and (d) 600 °C.

Figure 2 shows the FT-IR spectra of the samples treated at different temperatures. The appearance of two distinctive bands at ca. 568 (ν_1) and 667 cm^{-1} (ν_2), originating from the stretching vibrations of the metal–oxygen bond, confirms the formation of the Co_3O_4 spinel oxide [43–45]. The ν_1 band is associated with OB_3 vibrations in the spinel lattice, where B denotes the Co^{3+} in an octahedral position, and the ν_2 band is attributed to the ABO_3 vibrations, where A denotes the Co^{2+} in a tetrahedral position [46–47]. With the decrease of the particle size, the two bands slightly shift to a lower wave number due to a large number of defects at the surface of the much smaller nanoparticles to weaken the Co–O bond strength. The redistribution of free electrons between the surface and the bulk results in a decrease of the bond force constant, and consequently absorption red shifts [30]. The band near 1382 cm^{-1} of the LPC-250 IR spectra suggests that the sample calcined at 250 °C was contaminated with some nitrate radical residues [46], which disappear in other samples calcined at higher temperature.

It is clear that the TEM images of the Co_3O_4 samples (figure 3) calcined at 250 and 300 °C show monodisperse and ultrafine particles with uniform size about 5–13 nm, which is generally consistent with the calculation from the broadening of powder diffraction peaks in X-ray patterns. The particles are apt to aggregate together randomly with increasing the calcination temperature. It

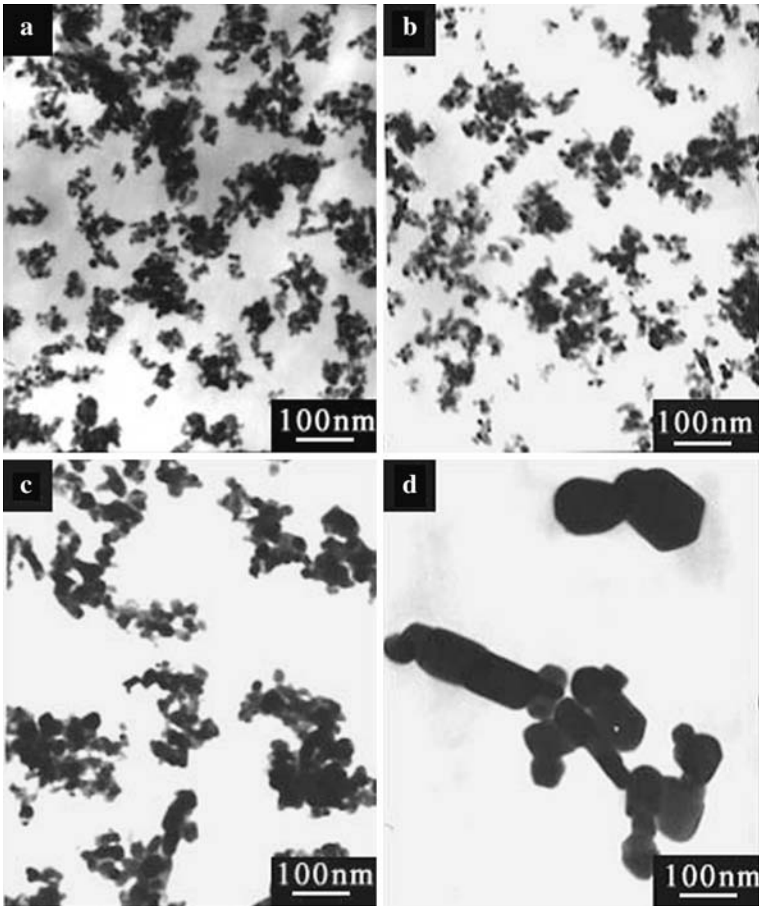

Figure 3. TEM images of Co_3O_4 catalysts calcined at different temperatures: (a) 250 °C; (b) 300 °C; (c) 400 °C and (d) 600 °C.

can be seen that there exists a certain extent of coagulation of the LPC-400, to a higher degree, of the LPC-600. The particle sizes estimated from TEM are presented in the fourth column of table 1.

Figure 4 shows the amount of active oxygen species, as obtained by CO titration and listed in the fifth column of table 1. The plot of active oxygen species shows a volcano curve with calcination temperature. The LPC-300 possesses the most amounts of active oxygen species. The same as the specific surface area, the amounts of active oxygen species decrease with increasing the calcination temperature. However, the LPC-250 possesses fewer amount of active oxygen species than that of the LPC-300, though the specific surface area of the former is slightly larger.

3.2. *Catalytic performance for low-temperature CO oxidation*

3.2.1. *Influence of calcination temperature on CO oxidation performance*

The CO oxidation performance of LPC-250, LPC-300, LPC-400 and LPC-600 as a function of reaction time is compared and given at room temperature in figure 5. It is evident that all the catalysts exhibit very high activity for CO oxidation at room temperature and the calcination temperature has a strong influence on the catalytic performance. However, the results are different from the reports presented by Jia [27], i.e. the high activity Co_3O_4 catalyst was obtained only under using DBS as the surfactant during the preparation process and being calcined at 300 °C. The results are also better than that of the literatures [28–30]. Under the similar pretreatment and reaction conditions, Lin *et al*. [28–29] and Wang *et al*. [30] reported that the full conversion of CO is reached at about 130 °C. It can also be observed that the reaction stability of CO oxidation increases gradually with the decrease of calcination temperature except 250 °C. The time of CO complete conversion is 50, 230, 500 and 240 min, respectively, listed in the last column of table 1.

Clearly, all the samples possess high catalytic activity existing as a pure Co_3O_4 phase with a spinel structure. However, the geometrical form and the particle size of Co_3O_4 are quite different for various catalysts. With increasing calcination temperature, the particles tended to aggregate and grow, which result in the decrease of the specific surface area, and the amount of active oxygen species on the samples. Hence, raising the calcination temperature results in a lower stability

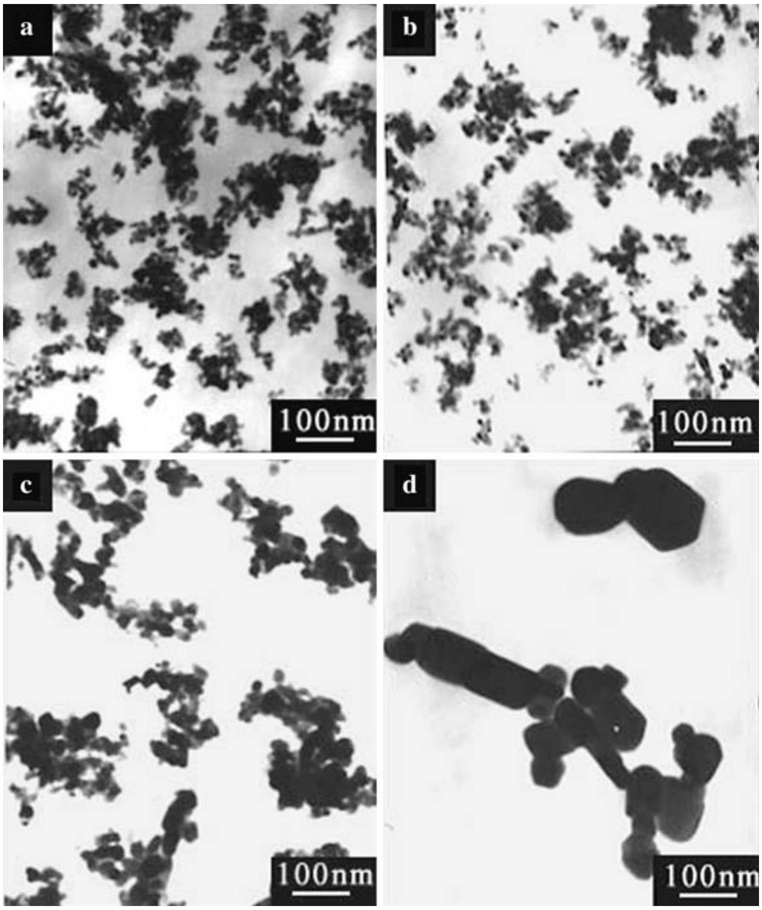

Figure 4. Effect of calcination temperature on the amount of active oxygen species on the Co_3O_4 catalysts.

(figure 5). However, the stability of CO oxidation over the LPC-250 is lower than that over the LPC-300, though the particle size of the former is smaller and the specific surface area is slightly larger. It should be noted that the amount of active oxygen species on the LPC-250 is fewer than that on the LPC-300, probably due to the presence of some nitrate radical residues on the surface of the LPC-250.

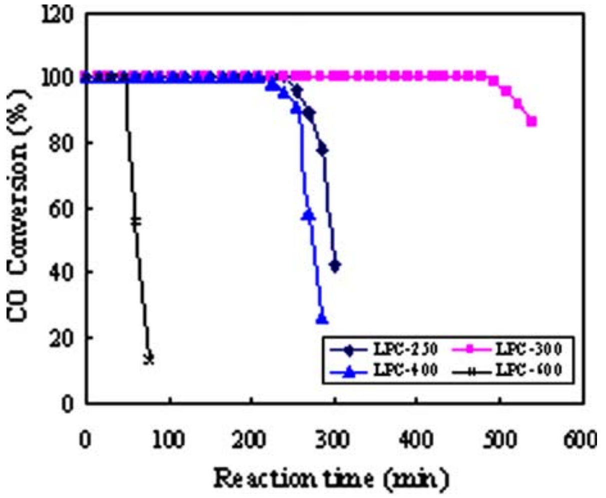

Figure 5. Catalytic performance of Co_3O_4 catalyst calcined at different temperatures (reaction conditions: CO 0.5%, O_2 14.4%, GHSV 5000 h^{-1}, room temperature.).

Jia *et al.* [27] reported that the particle size of Co_3O_4 catalysts was crucial to the catalytic performance for low-temperature CO oxidation. Lin *et al.* [28] found that the catalytic activities toward the CO oxidation were decreased significantly with the oxidation state of cobalt, i.e. $CoO(+2) \geq Co_3O_4(+8/3) \gg CoO(OH)(+3) \geq CoO_x(>+3)$, and Wang *et al.* [30] reported that the T_{50} was decreased significantly with increasing the S_{BET} of the Co_3O_4. With the increase of calcination temperature, unlike the trend of particle size and specific surface area, the amount of active oxygen species showed a volcano curve. This indicates that the amount of active oxygen species is one of the main factors which affect the catalytic performance.

3.2.2. *Influence of reaction temperature on CO oxidation*

Figure 6 shows the CO oxidation performance of the LPC-300 catalyst as a function of reaction time at various reaction temperatures, which are −78, −20, 0, 25 and 50 °C, respectively. Apparently, the catalyst showed very high activity for CO oxidation at low temperature and it was able to maintain its activity for CO complete

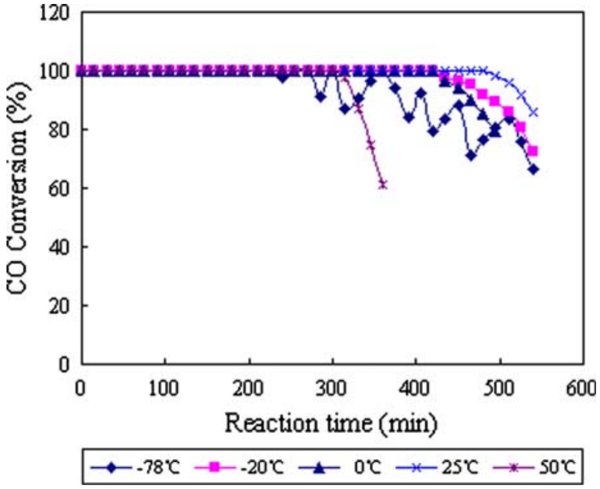

Figure 6. Catalytic performance of the LPC-300 catalyst at different reaction temperatures (reaction conditions: CO 0.5%, O_2 14.4%, GHSV 5000 h^{-1}).

oxidation at −78 °C about 240 min followed by periodic oscillations of CO conversion, just as the result reported by Cunningham [31]. The most probable explanation is the intermittent decomposition of carbonate intermediates at the catalyst surface. It can be seen that the stability of the LPC-300 catalyst increases with increasing reaction temperature from −78 to 25 °C, though the difference of the stability at −20 and 0 °C is not obvious. The results are better than that of the literatures, and the T_{50} is −54, 80, and −63 °C [31–32, 34], respectively. However, raising the reaction temperature to 50 °C, the time of CO complete conversion decreased compared to that of 25 °C. This is, perhaps, related to the strong thermal release originated from the CO oxidation, and the further investigation is still under discussion.

4. Conclusions

Without use of any surfactant or oxidant, a series of Co_3O_4 catalysts with a high catalytic activity were prepared by a very simple liquid-precipitation method. It can be seen that all the samples calcined at different temperatures exist as a pure Co_3O_4 phase with the spinel structure. The samples calcined at 250 and 300 °C show monodisperse and ultrafine particles with the particle size being 5–13 nm. The particles tend to aggregate and the average size increases gradually with increasing the calcination temperature from 250 to 600 °C, and the specific surface area decreases from 61 to 9 m^2g^{-1}. Particularly, the sample obtained at 250 °C is contaminated with some nitrate radical residues which disappear at other samples calcined at higher temperature. The present preparation method is facile, inexpensive and practical in scale up.

The samples are very effective for the low-temperature CO oxidation. The catalytic stability of the sample toward CO oxidation increases with decreasing calcination temperature from 600 to 300 °C due to the decrease of the average particle size and the increase of the specific surface area. CO titration experiments show that the amount of active oxygen species on the samples appears to be critical for catalytic performance. The LPC-300 possesses the most amounts of active oxygen species and shows the highest catalytic stability compared to that of other samples. The LPC-300 is able to maintain its activity for CO complete oxidation more than 500 min at 25 °C and about 240 min even at −78 °C. Compared with Co_3O_4 catalyst reported in the literatures, our catalysts exhibit better low-temperature catalytic performance.

Acknowledgments

The authors thank the Shanxi Natural Science Foundation (grants: 20041017) and Shanxi Scientific & Technological Promoted Project of China (grants: 031099) for the financial support of this work.

References

[1] S.D. Gardner, G.B. Hoflund, B.T. Upchurch, D.R. Schryer, E.J. Kielin and J. Schryer, J. Catal. 129 (1991) 114.
[2] A.B. Lamb, W.C. Bray and J.C.W. Frazer, Ind. Eng. Chem. 12 (1920) 213.
[3] H. Yamaura, K. Moriya, N. Miura and N. Yamazoe, Sens. Actuators B 65 (2000) 39.
[4] N. Funazaki, Y. Asano, S. Yamashita, T. Kobayashi and M. Haruta, Sens. Actuators B 13–14 (1993) 536.
[5] A.K. Tripathi, N.M. Gupta, U.K. Chatterji and R.M. Iyer, Indian J. Technol. 30 (1992) 107.
[6] P. Thormählen, E. Fridell, N. Cruise, M. Skoglundh and A. Palmqvist, Appl. Catal. B 31 (2001) 1.
[7] M. Shelef and R.W. McCabe, Catal. Today 62 (2000) 35.
[8] D.H. Kim and M.S. Lim, Appl. Catal. A 224 (2002) 27.
[9] P.V. Snytniko, V.A. Sobyanin, V.D. Belyaev, P.G. Tsyrulniko, N.B. Shitova and D.A. Shlyapin, Appl. Catal. A 239 (2003) 149.
[10] G.L. Dong, J.G. Wang, Y.B. Gao and S.Y. Chen, Catal. Lett. 58 (1999) 37.
[11] Y.U. Bi and G.X. Lu, Appl. Catal. B 41 (2003) 279.
[12] P. Bera, A. Gayen, M.S. Hegde, N.P. Lalla, L. Spadaro, F. Frusteri and F. Arena, J. Phys. Chem. B 107 (2003) 6122.
[13] J.L. Margitfalvi, I. Borbáth, M. Hegedűs, E. Tfirst, S. Gőbölös and K. Lázár, J. Catal. 196 (2000) 200.
[14] Daniel M.C., Astruc D. Chem. Rev. 104 (2004) 341, and references cited therein.
[15] M.L. Jia, Y.N. Shen, C.Y. Li, Z.R.G.T. Bao and S.S. Sheng, Catal. Lett. 99 (2005) 235.
[16] M.Á. Centeno, C. Portales, I. Carrizosa and J.A. Odriozola, Catal. Lett. 102 (2005) 289.
[17] A. Jain, X. Zhao, S. Kjergaard and S.M. Stagg-Williams, Catal. Lett. 104 (2005) 191.
[18] F. Moreau and G.C. Bond, Catal. Today 114 (2006) 362.
[19] Moreau F., Bond G.C., Taylor A.O. (2004) Chem. Comm. 1642.
[20] C.W. Chiang, A.Q. Wang, B.Z. Wan and C.Y. Mou, J. Phys. Chem. B 109 (2005) 18042.
[21] M.F. Luo, Y.J. Zhong, X.X. Yuan and X.M. Zheng, Appl. Catal. A 162 (1997) 121.

[22] G.J. Hutchings, A.A. Mirzaei, R.W. Joyner, M.R.H. Siddiqui and S.H. Taylor, Appl. Catal. A 166 (1998) 143.
[23] S.H. Taylor, G.J. Hutchings, A.A. Mirzaei (1999) Chem. Comm. 1373.
[24] D.M. Whittle, A.A. Mirzaei, J.S.J. Hargreaves, R.W. Joyner, C.J. Kiely, S.H. Taylor and G.J. Hutchings, Phys. Chem. Chem. Phys. 4 (2002) 5915.
[25] C.M. Bae, J.B. Ko and D.H. Kim, Catal. Comm. 6 (2005) 507.
[26] Y. Yu and F. Yung, J. Catal. 33 (1974) 108.
[27] M.J. Jia, W.X. Zhang, Y.G. Tao, G.Y. Wang, X.H. Cui, C.L. Zhang and T.H. Wu, Chem. J. Chin. Univ. 20 (1999) 637(in Chinese).
[28] H.K. Lin, H.C. Chiu, H.C. Tsai, S.H. Chien and C.B. Wang, Catal. Lett. 88 (2003) 169.
[29] H.K. Lin, C.B. Wang, H.C. Chiu and S.H. Chien, Catal. Lett. 86 (2003) 63.
[30] C.B. Wang, C.W. Tang, S.J. Gau and S.H. Chien, Catal. Lett. 101 (2005) 59.
[31] D.A.H. Cunningham, T. Kobayashi, N. Kamijo and M. Haruta, Catal. Lett. 25 (1994) 257.
[32] J. Jansson, J. Catal. 194 (2000) 55.
[33] J. Jansson, E.C.P. Anders, E. Fridell, M. Skoglundh, L. Österlund, P. Thormählen and V. Langer, J. Catal. 211 (2002) 387.
[34] P. Thormählen, M. Skoglundh, E. Fridell and B. Andersson, J. Catal. 188 (1999) 300.
[35] X.C. Zheng, S.H. Wu, S.P. Wang, S.R. Wang, S.M. Zhang and W.P. Huang, Appl. Catal. A 283 (2005) 217.
[36] Y.Z. Chen, B.J. Liaw and C.W. Huang, Appl. Catal. A 302 (2006) 168.
[37] M. Krämer, T. Schmidt, K. Stöwe and W.F. Maier, Appl. Catal. A 302 (2006) 257.
[38] R.S. Drago, K. Jurczyk, D.J. Singh and V. Young, Appl. Catal. B 6 (1995) 155.
[39] E.V. Steen and H. Schulz, Appl. Catal. A 186 (1999) 309.
[40] Z.L. Zhang, H.R. Geng, L.S. Zheng and B. Du, J. Alloys. Compd. 392 (2005) 317.
[41] K. Schmidt-Szaowski, K. Krawczyk and J. Petryk, Appl. Catal. A 175 (1998) 147.
[42] J.I. Langford and A.J.C. Wilson, J. Appl. Crystallogr. 11 (1978) 102.
[43] J.A. Gaddsden, *Infrared spectra of minerals and related inorganic compounds* (Butterworth, London, 1975) 44.
[44] C. Spenser and D. Schroeder, Phys. Rev. B 9 (1974) 3658.
[45] T. Andrushkevich, G. Boreskov, V. Popovskii, L. Pliasova, L. Karakchiev and A. Ostankovitch, Kinet. Katal. 6 (1968) 1244.
[46] St.G. Christoskova, M. Stoyanova, M. Georgieva and D. Mehandjiev, Mater. Chem. Phys. 60 (1999) 39.
[47] R.N. Singh, J.P. Pandey, N.K. Singh, B. Lal, P. Chartier and J.F. Koenig, Electrochim. Acta. 45 (2000) 1911.